Energy Conversion and Management: X 13 (2022) 100175

Contents lists available at ScienceDirect

Energy Conversion and Management: X

journal homepage: www.sciencedirect.com/journal/energy-conversion-and-management-x

On the tuning and performance of Stand-Alone Large-Power PV irrigation systems

Juan Ignacio Herraiz [a,b,*], José Fernández-Ramos [c], Rita Hogan Almeida [a], Eva María Báguena [a], Manuel Castillo-Cagigal [b], Luis Narvarte [a]

[a] Instituto de Energía Solar - Universidad Politécnica de Madrid, C/Nicola Tesla s/n, 28031 Madrid, Spain
[b] Qualifying Photovoltaics, C/Alan Turing 1, 28031 Madrid, Spain
[c] Departamento de Electrónica, Universidad de Málaga, 29071 Málaga, Spain

ARTICLE INFO

Keywords:
Water pumping
PV irrigation system
Frequency converter
Stand-alone PV system

ABSTRACT

Stand-alone large-power PV irrigation systems without batteries is a recent innovation. This means that their design has not yet reached maturity and there are no experimental data about their performance available. This paper is a contribution, on the one hand, to the systematic tuning of the control of this type of systems and, on the other hand, to the knowledge of their experimental performance data.

A systematic Proportional, Integral and Derivative (PID) control tuning method for frequency converters is proposed, based on the application of the Approximate M−constrained Integral Gain Optimisation (AMIGO) design rules to the frequency response tuning method, and applied to two PV irrigation systems, located respectively in Villena and Aldeanueva de Ebro, Spain, that had a "conservative" tuning by means of an experimental trial and error method.

To check the goodness of this systematic tuning, the experimental performance of both systems has been evaluated from 2017 to 2021. New indices have been proposed to assess both the robustness of the system to PV power fluctuations (the "Number of abrupt stops" and the "Passing-cloud resistance ratio") and the performance (by factoring the traditional Performance Ratio (*PR*) to determine the influence of different factors external to the system). Results show that the percentage of abrupt stops improves from 40% and 39.8% in each PV irrigation system prior to systematic tuning to 7.3% and 1.3% after tuning; the passing cloud ratio increases from 65% and 79% to 97.9% and 99.8% and the *PR* from 61.4% and 60% to 65.7% and 64.7%.

Introduction

The technology of stand-alone large-power photovoltaic (PV) irrigation systems without batteries is relatively recent, driven by rising energy costs in modernized agriculture [1–3]. Until recently, this type of system was restricted to plug-and-play kits consisting of a PV generator, a frequency converter (FC) and an alternating current centrifugal motor pump [4–6], with a maximum power of 40 kWp. The reason for this power limitation was the impossibility of ensuring the stability of the control of the FC due to the variability of the PV power, which resulted in sudden stops of the FC that produced water hammer in the hydraulic system and overvoltages between the FC output and pump motor [7–9]. This problem was solved by integrating batteries [10–12], but their high cost, even for new accumulation technologies such as those based on phase change materials [13,14] was again a reason for not being able to increase the power of the systems.

In the last decade, new control algorithms have been developed that, taking advantage of the regeneration capacity of centrifugal motor pumps, solve control instabilities and their associated problems [15]. In addition, trackers with a horizontal north–south axis were incorporated to adjust the PV production throughout the year to the irrigation needs and to produce quasi-constant PV power profiles that better adjust to the dynamics of the water sources [16–18]. Communication protocols were developed to integrate control of PV irrigation systems and irrigation controllers to make it easier for farmers to embrace the innovation. Fixed support structures for the PV generator called "delta" were also proposed which, thanks to their east–west orientation, also produce constant power profiles [19]. These solutions were integrated into five full-scale demonstrators in real irrigation infrastructures of farmers,

* Corresponding author at: Qualifying Photovoltaics, C/Alan Turing 1, 28031 Madrid, Spain.
E-mail addresses: ji.herraiz@upm.es (J.I. Herraiz), josefer@ctima.uma.es (J. Fernández-Ramos), rita.hogan@upm.es (R. Hogan Almeida), eva.baguena@upm.es (E.M. Báguena), m.castillo@qpv.es (M. Castillo-Cagigal), luis.narvarte@upm.es (L. Narvarte).

https://doi.org/10.1016/j.ecmx.2021.100175
Received 1 October 2021; Received in revised form 9 December 2021; Accepted 29 December 2021
Available online 3 January 2022

Nomenclature

AC	Alternating Current
AMIGO	Approximate M−constrained Integral Gain Optimisation
cum	Cumulative
DC	Direct Current
E_{PV}	PV Energy (Wh)
FC	Frequency Converter
G	Effective solar irradiance in the plane of the PV generator (W/m^2)
G_{max}	Minimum irradiance that allows the PV generator to provide the maximum power that the pump can consume at a given cell temperature (W/m^2)
G_{md}	Midday irradiance in the equinox (W/m^2)
G_{start}	Minimum irradiance needed to reach the power threshold (W/m^2)
G_{stop}	Minimum irradiance level under which the FC cannot be running (W/m^2)
G_{used}	Used irradiance (W/m^2)
G_{useful}	Useful irradiance (W/m^2)
G_{wasted}	Wasted irradiance (W/m^2)
G^*	Irradiance at standard test conditions (W/m^2)
I_{AC}	AC current (A)
I_{DC}	DC current (A)
IAE	Integral Absolute Error
IAFE	Integral Absolute Frequency Error
IP	Irrigation Period
K_c	Critical gain
K_p	Proportional gain
l	Smallest dimension of the perimeter of the PV generator (m)
MPP	Maximum Power Point
MPPT	Maximum Power Point Tracking
P_{AC}	AC Power (W)
PID	Proportional Integral Derivative
PLC	Programmable Logic Controller
PR	Performance Ratio (%)
PR_{PV}	Photovoltaic PR (%)
PV	Photovoltaic
PVIS	PV Irrigation System
P^*	Peak power of the PV generator (Wp)
T	Time (s)
t_{acel}	Acceleration time (s)
T_c	Cell temperature (°C)
T_{crit}	Critical period (Hz)
T_i	Integral time (s)
UR_{EF}	Effective Utilization Ratio: ratio of the irradiation required to keep P_{AC} stable during the irrigation scheduling to the same irradiation during the IP (%)
UR_{IP}	IP Utilization Ratio: ratio of the total irradiation throughout the irrigation period to the total annual irradiation (%)
UR_{PVIS}	PVIS Utilization Ratio: ratio of the irradiation strictly required to keep P_{AC} equal to the stable AC power requirement to the total irradiation throughout the IP (%)
V_{AC}	AC voltage (V)
V_{DC}	DC voltage (V)
V_{DCmin}	Minimum DC voltage (V)
V_{OC}	Open-circuit voltage (V)
V_{sp}	Setpoint voltage (V)
$\eta_{DC/AC}$	FC efficiency (%)
η_P	Real power versus nominal power of the PV generator (%)
η_T	Thermal efficiency of the PV generator (%)
σ_{cloud}	Passing-cloud resistance ratio (%)

irrigation communities and agro-industries in Spain, Portugal, Italy and Morocco in the context of an European project to demonstrate their technical reliability and economic and environmental viability [20–24]. But its character of recent technology means that it has not yet reached maturity in its design and that there is no experimental data that allows us to know the performance that can be expected from this type of system.

Regarding the design, the state of the art of the tuning of the PID control of the FC is based on trial and error procedures that must be carried out in-situ given the influence of the hydraulic system to which the PV irrigation system is connected to. These trial and error procedures do not allow optimal performance of PV irrigation systems to be achieved. There are no automatic procedures for this tuning since the existing ones are for linear and invariant systems [25–33] but in PV irrigation systems the relationship between the control variable (PV generator voltage) and the output variable (pump rotation frequency) is non-linear and dependent on irradiance and temperature, that is, variable with time. Some studies have been published that address this problem [34,35]. They have been carried out on small laboratory facilities where it is feasible to control some of the variables that decisively influence the control of large-power PV irrigation systems in their three relevant operating zones: operation at high and constant irradiance values (clear day) [34]; the fast response to sudden changes in irradiance (passing of clouds over the PV generator) [35]; and start-up [35], a process by which the pump goes from standstill to the highest possible frequency in a very short time, typically in less than two seconds. The fundamental problem is that the optimization of the performance in some of these operating regions usually causes a deterioration in the operation in the others.

Regarding performance, there are several publications that report on the overall system efficiency of PV pumping systems. For example, [36] reports 5% and 7% for systems that use diaphragm and helical pumps, respectively; [37] reports an overall efficiency of 2.5% with an optimal water flow rate of 2.7 m^3/h; [38] reports 1.299% without shading and 0.83% with shading and [39] reports a best system efficiency at low solar irradiation of 7% for a 50 m pumping head and 6.6% at high solar irradiation for a 80 m pumping head. But it is necessary to underline that, unlike grid-connected PV systems, in which their performance depends basically on the quality of the system itself, in PV irrigation systems there are external factors that affect their performance, even though the quality of the system is good: the irrigation period of the crop (usually less than the full year), the characteristics of the irrigation infrastructure to which it is connected (which does not allow to take advantage of all the available irradiation, for example, because the pump cannot work above its nominal frequency) or the behavior of the irrigator [21]. Performance indices have been proposed that factor the traditional Performance Ratio (PR) [40] into various utilization ratios that quantify the influence of these external factors on system performance [21]. However, there is still no information available in the literature on experimental performance data that allow to know what is the expected performance in this type of systems.

The novelty of this paper is that it proposes a systematic tuning method that takes into account the three operating zones of PV irrigation systems. This method has been applied to the tuning of two real large-power PV irrigation systems that were already in operation and had been tuned through a trial and error procedure. To assess the goodness of this new tuning method, the performance of these two systems has been evaluated from 2017 to 2021, before and after tuning, not only

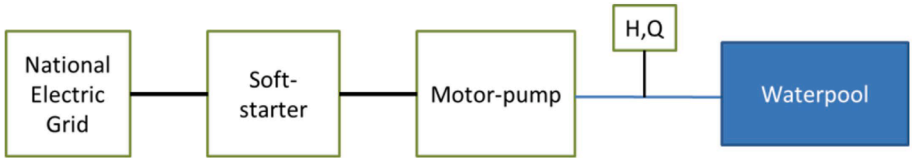

Fig. 1. Pre-existent irrigation system configuration: The electric power from the national electric grid guarantees that the motor-pump will always work at 50 Hz (system monitors both water height – H– and flow – Q).

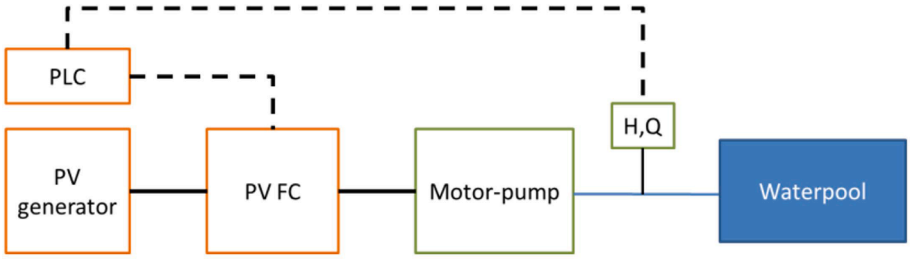

Fig. 2. PV irrigation system configuration: The PV generator substitutes the national grid and the FC the soft-starter. A PLC has been added to the pre-existent configuration. New components are marked in orange. Components that remain from the previous system are in green. (For interpretation of the references to colour in this figure legend, the reader is referred to the web version of this article.)

Fig. 3. PV irrigation system in Villena.

under stable irradiance conditions but also under conditions of fluctuating PV power. Therefore, this paper provides experimental performance data, which opens the door to the knowledge of the expected performance in stand-alone large-power PV irrigation systems without batteries and pumping to an elevated water pool. This is key to establish quality thresholds in technical specifications and quality control procedures in the context of contractual frameworks for the sale and installation of this type of systems.

Methodology

Description of the PV irrigation systems under study

Villena irrigation system

The pre-existing system. The system is located in the "San Cristóbal" borehole of the Irrigator Community of Alto Vinalopó, in Villena, Alicante, Spain (38°41'16''N, 0°50'33''W). The pre-existing system is schematized in Fig. 1 and was composed by a 250 kW submersible centrifugal motor-pump (Caprari - E12S55FUS/10A + MAC 12,340 /1C/DF/V-8) powered by the national grid. It pumps water from a 400 m deep-borehole to a water pool of 173,000 m^3, elevated 12 m from the ground. The pump is installed at a depth of 300 m, the dynamic level of the water in the well is 257 m and the total manometric head is 269 m.

The new PV irrigation system. The new PV irrigation system (PVIS) was designed to totally substitute the grid. The size of the PV generator was selected so that on clear days, at midday on the equinox days, the system is able to work at its maximum AC power (P_{AC}) [21]. The PV peak power of the PV generator (P^*) [40] is defined as $P^* = (P_{AC} \times G^*)/(G_{md} \times \eta_P \times \eta_T \times \eta_{DC/AC})$, where $G^* = 1000 W/m^2$, G_{md} is the midday irradiance in the equinox, η_P is the real power versus the nominal power of the PV generator (which includes the losses due to mismatching, dirtiness, and ageing of the PV generator), η_T is the thermal efficiency of the PV generator, and $\eta_{DC/AC}$ is the efficiency of the FC. In this particular case, P_{AC} is 240 kW and $\eta_{DC/AC}$ is 0.98, according to datasheet. Reasonable values for η_P and η_T are 0.96 and 0.9 respectively. This leads to P^*= 362 kWp. For reasons of modularity, the final P^* was established as 360 kWp. The PV modules were mounted in two different types of trackers: two STI-H1250 (single axis multi row tracker) with 8 rows each and two STI-H160 (single row). The PV system is composed by 1440 PV modules (M Prime 3R PLUS of 250 Wp) that are connected in 72 strings of 20 modules. This system includes a FC of 355 kW (OMRON A1000 CIMR-AC4A0675AAA), able to transform the direct current (DC) generated by the PV modules to alternating current (AC) at a variable frequency, allowing the pump to work at different frequencies according to the available PV power. The system also includes an external Programmable Logic Controller, PLC, (OMRON CP1L-M40D) to control the system. A schematic of the new PVIS configuration can be seen in Fig. 2 and an aerial view of the system (PV generator, water pool and borehole) in

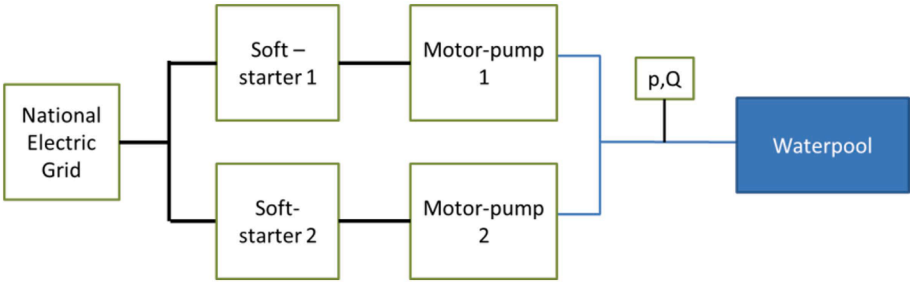

Fig. 4. Pre-existent irrigation system configuration: The electric power from the national electric grid keeps the output frequency at 50 Hz (system includes the measurement of both water pressure, p, and flow, Q).

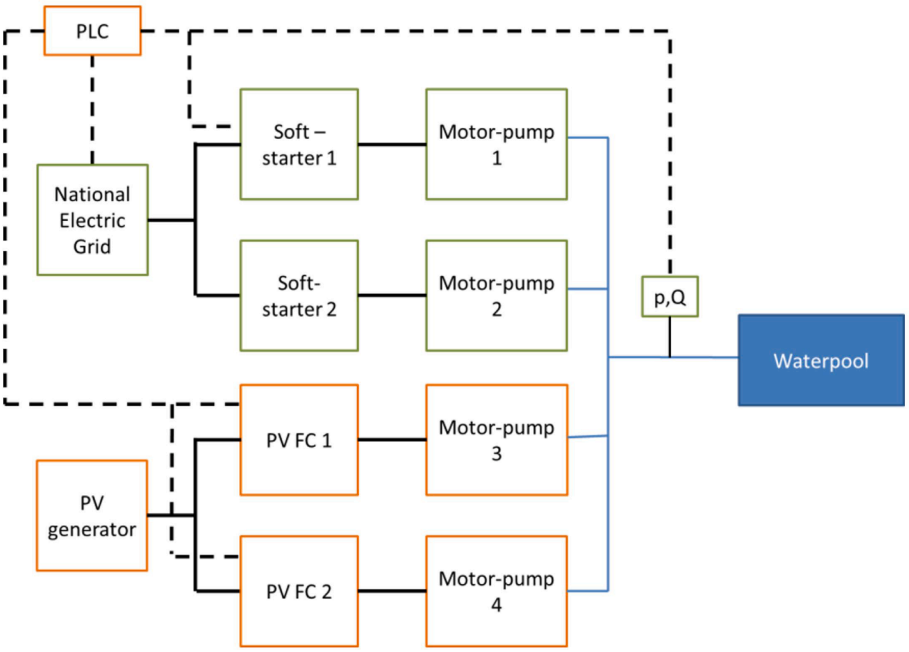

Fig. 5. PV irrigation system configuration: A PV generator, two FCs, two motor-pumps, and a PLC have been added to the pre-existent configuration. New components are marked in orange. Pre-existing components are in green. (For interpretation of the references to colour in this figure legend, the reader is referred to the web version of this article.)

Fig. 3.

Regarding the control of the system, the PLC is always estimating the available PV power, through the measurement of the irradiance on the plane of the PV generator and cell temperature from a reference cell (ATERSA MU-68-D) installed on the tracker. Once this estimated PV power is greater than a threshold that allows the pump to work, the PLC gives the run signal to the FC and the system starts pumping to the water pool. At the end of the day, the system stops once the estimated power is under a power threshold or the output frequency is below the minimum frequency (38 Hz), in which the system is able to elevate water to the pool, during a minute.

The system is monitored by means of one-second records of: effective solar irradiance in the plane of the PV generator (G); cell temperature (T_c); output frequency of the FC, DC voltage (V_{DC}) and current (I_{DC}) at the input of the FC; AC voltage, current and power at the output of the FC (V_{AC}, I_{AC} and P_{AC} respectively); water flow; and water level in the borehole. Commissioning tests were carried out after the PV system was set up in 2016. During the commissioning, the start and stop thresholds for power and frequency were adjusted and the tuning of the PID control of the FC was done "conservatively" to ensure stable operation under "normal" operating conditions (high and stable irradiance values), using an experimental trial and error method that provided values of $K_p = 0{,}23$; $T_i = 0{,}4$ s, where K_p is the proportional gain and T_i is the integral time (the derivative parameter is not used due to the high electrical noise of the FC).

Aldeanueva irrigation system

The pre-existing system. The system belongs to the Irrigator Community of "Las Planas" and is located in Aldeanueva de Ebro, La Rioja, Spain (42°11'50.9''N, 1°49'58.0''W). The Community has almost 100 farmers who represent 246 ha of irrigated vineyards. The pre-existing system (Fig. 4), with two vertical inline centrifugal pumps, was powered by the national grid. Each pump of 75 kW is able to elevate 54 m^3/h of water from Lodosa Channel to a 70,000 m^3 water pool located 8 km away, with a total manometric head of 225 m.

The new PV irrigation system. To avoid electricity consumption in high price periods, the decision was to install two more pumps (KSB BEV-8400/11) only powered by PV. The idea is to pump the maximum volume of water during the day with the PV system, and only use the previous pumps, fed by the grid, during night time to compensate some spikes in water demand (usually, the second fortnight of July and the first of August). A PV generator of 213 kWp feeds both pumps and is installed in a North-South horizontal axis tracker (Nclave SP160) of ten rows with 600 PV modules (TwinPeak 2S 72 SERIES - REC Solar of

Fig. 6. Aerial view of PV irrigation system in Aldeanueva.

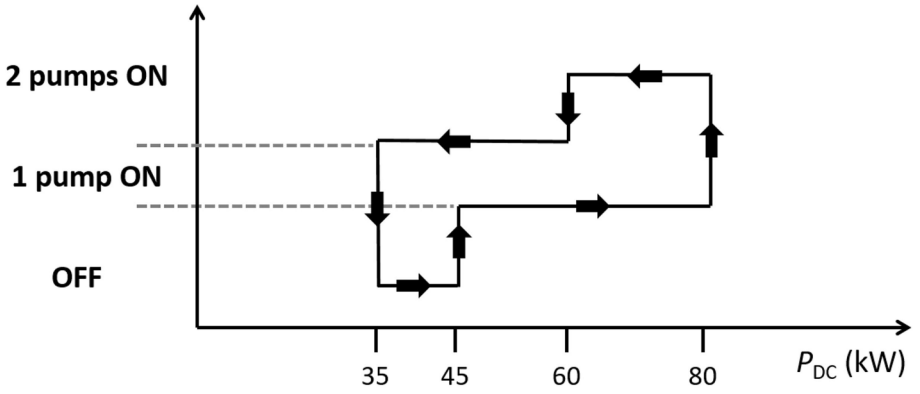

Fig. 7. Available PV power thresholds with hysteresis for start and stop of the pumps.

355Wp) that are connected in 40 strings of 15 modules in series. The system includes two frequency converters (FCs) of 110 kW (OMRON RX 110 kW − 3G3RX-B411K-E1F) and an external PLC (composed by two Siemens 6ES7131-6BH00-0BA0, a Siemens 6ES7132-6BH00-0BA0 and a Siemens 6ES7134-6GD00-0BA1). Fig. 5 shows the configuration of the system and Fig. 6 shows an aerial view of the PVIS in Aldeanueva.

The control of the start and stop of each pump is done by the PLC, which has four PV power thresholds (see Fig. 7). When the estimated PV power is greater than or equal to 45 kW, a run command is given to one of the FCs and its pump starts operating. The corresponding FC executes the maximum power point tracking (MPPT) routine. The second pump starts when the estimated PV power is greater than 80 kW. Both pumps work at the same output frequency in a master–slave control mode. Each day the master-pump is the one with less operation hours (this is key for maintenance tasks since this way both pumps always have more or less the same working hours).

The system is monitored by means of one-second records of: G, T_c, output frequency, set point frequency, V_{DC}, I_{DC}, and I_{AC} of both FCs, water flow and pressure. The commissioning of this system was done at the end of July 2018 and the PID tuning of the FC was done "conservatively" to ensure stable operation under "normal" operating conditions by means of an experimental trial and error method that provided values of $K_p = 0.2$ and $T_i = 0.1$ s.

"Systematic" tuning method

After a period of time in which the systems were operating with the parameters obtained experimentally in the commissioning, a new PID tuning of the FCs was carried out applying the methodology developed by Fernández-Ramos et al. [35]. These tests were carried out on February the 4th, 2020 in Villena and on September the 26th, 2019 in Aldeanueva. The results of this tuning were optimized by applying two different methods for the fine adjustment of PID control parameters, one in each installation.

Application of the AMIGO method

The tuning was carried applying the AMIGO design rules to the frequency response tuning method [25]. In this method, sustained uniform oscillations are caused both in the operating frequency of the pump and in the voltage of the PV generator. The value of K_p at which this oscillation occurs is called the "critical gain" (K_c) and the period of the oscillation is called the "critical period" (T_{crit}). These values are used by the AMIGO design rules to calculate the appropriate control values, K_p and T_i. The main problem when applying this method to PVIS is that to obtain K_c it is necessary to take the system to the stability limit without exceeding it, so that a sudden stop of the pump does not appear. Two parameters make it difficult to obtain a stable oscillation in PVIS:

- The acceleration time (t_{acel}) set in the FC. To improve the control in normal operation, it must be set to the smallest value allowed by the FC [35]. But, as the power of the PVIS to be tuned increases, very small t_{acel} values make it almost impossible to obtain a stable oscillation.
- The control setpoint voltage (V_{sp}), which in normal operation is the PV generator's maximum power point (MPP) voltage. At this working point, the derivative of the generator's power-voltage curve is null, making it very difficult to obtain a stable oscillation. This makes it necessary to set a setpoint higher than the MPP voltage.

In short, under normal operating conditions, V_{sp} must be the MPP

voltage and t_{acel} must be as small as possible, but it is not possible to perform a tuning by the frequency response method in these conditions.

To overcome this drawback, tuning tests have been carried out for different V_{sp} and t_{acel} values and relationships have been sought that allow these results to be extrapolated to the normal operating conditions of the system. These tests have been performed in the laboratory system described in [35] with the following conclusions:

- T_{crit} is approximately constant, with a slight downward trend as t_{acel} increases.
- K_{c} increases as V_{sp} increases, although the product of $(V_{OC}$ - $V_{sp}) \cdot K_{\text{c}}$ is approximately constant.
- K_{c} increases slightly as t_{acel} increases.
- K_{c} at the value of V_{sp} corresponding to the MPP can be calculated as $K_c = 1/(V_{OC} - V_{sp}(MPP)) \cdot (\sum_{i=1}^{n} (V_{OC} - V_{spi}) \cdot K_{ci})/n$

Therefore, it can be concluded that it is possible to tune the system under more favorable conditions to obtain a stable oscillation (values of t_{acel} and V_{sp} higher than necessary for the normal operation of the system) and, later, adjust K_{c} and T_{crit} values to approximate what they would have if the tuning had been done under normal operating conditions. Once the adjusted values of K_{c} and T_{crit} have been obtained, the AMIGO tuning rules are applied to obtain the appropriate values of the K_{p} and T_{i} system control parameters.

Fine adjustment of control parameters

To confirm the suitability of the K_{p} and T_{i} parameters obtained by the tuning method described above, the system performance has been evaluated at start-up and passing-cloud transition [35]. The start-up test consists of setting V_{sp} as the MPP voltage and starting the system. The figures of merit of this test are the time elapsed until reaching the setpoint (the shorter the better) and the minimum voltage that the PV generator reaches during the transient (V_{DCmin}) (the higher the better). Regarding passing-cloud tests, two types of tests have been designed depending on whether there are one or more pumps in the PVIS. The objective of these tests is to emulate the sudden drop in power supplied to the pump when a passing cloud progressively covers the PV generator.

a) Method for PVIS with more than one pump connected to the PV generator.

This method was applied to the Aldeanueva facility, equipped with two identical pumps, each controlled by its own FC that can be started independently. The procedure consists of making pump 1 work with a V_{sp} equal to the MPP voltage and configured with the K_p and T_i parameters to be tested. Initially, pump 2 is off or running at a certain fixed frequency, without performing any PID control. Once pump 1 is running, pump 2 is accelerated to a higher frequency value, with a predetermined slope. This acceleration consumes power from the PV generator, and pump 1 suffers a sudden drop in its available PV power, similar to what happens when a cloud covers the generator. The generator voltage suffers a sudden drop, which must be counteracted by the control system of pump 1 by means of a rapid drop in its operating frequency, forcing the voltage to return to its setpoint value. The generator voltage and the operating frequency of pump 1 must be monitored. The figures of merit for evaluating the performance of a given set of K_p and T_i parameters are:

- Robustness against voltage drop in the PV generator: evaluated by measuring V_{DCmin} during the transient (the higher the better).
- Process energy efficiency: evaluated by comparing the curve of the evolution of the pump real frequency with the ideal curve that it should follow. The smaller the area between these two curves, the better, since this indicates a better use of the energy available in the PV generator. This is called Integral Absolute Frequency Error (IAFE).

b) Method for systems with a single pump (Feedforward method).

As the method described above cannot be applied to systems where there is a single pump connected to the generator, such as Villena PVIS, a method based on the use of a PID controller with a "feedforward" input is used. The feedforward design is a very widespread powerful technique that basically consists of adding a signal to the output of the controller, so that the operating frequency of the pump is obtained by adding the output of the PID controller to the feedforward signal. The feedforward input of the FC is connected to a pulse generator in which both the voltage levels and the slope can be configured. This signal sets the frequency value that is added to the output of the PID controller to obtain the final operating frequency of the pump. Initially, the feedforward signal is null, so the PID controller output is the pump operating frequency. After this, a feedforward signal is applied. The amplitude of this signal must be such that the maximum operating frequency of the pump is not exceeded. Its slope is established as a function of the irradiance gradient of the cloud to be simulated.

The injection of this signal causes an increase in the operating frequency of the pump, which provokes a sudden drop in the generator voltage, because it cannot provide the necessary power for this increase in frequency, since it is operating at the MPP. This voltage drop must be counteracted by the PID controller, which must rapidly decrease its output so that the operating frequency of the pump decreases and the generator voltage returns to its setpoint. From the point of view of the PID controller, it seems as if the available power of the PV generator drops abruptly, similarly to what happens when a cloud passes over it.

The PV generator voltage and the PID controller output are monitored. This type of test allows many more tests to be carried out, so the fundamental figure of merit is the steepest feedforward signal slope that is capable of withstanding a given set of K_p and T_i parameters, without triggering an undervoltage alarm. The second figure of merit to consider is V_{DCmin}. Finally, the IAFE is not evaluated because the behavior of the frequency in this test is different from the behavior in the test described above. Instead, the standard integral absolute error (IAE) on the PV generator voltage is evaluated.

Fine tuning adjustment is implemented by carrying out these tests both on the set of parameters obtained in the tuning process and on other sets of parameters that present small variations around it, in order to determine the most appropriate set of parameters.

Indicators used to assess the PVIS tuning and performance in real operating conditions

In order to analyse and assess the quality of the system tuning, new performance indices have been described.

Number of abrupt stops

A FC stop is considered to be "abrupt" when it occurs suddenly and with no control, and "controlled" when the PLC or the FC itself initiates it and is performed gradually. Under normal operating conditions, FCs must stop in a controlled way. Nevertheless, large-power PVIS control instabilities, caused either by PV power quick intermittences or by a malfunction of the control system, can lead on to abrupt FC stops that cause water hammer and AC overvoltages that seriously threaten the integrity of the hydraulic and electric components of the PVIS. A large number of abrupt stops will pose a greater risk of breakdowns. On the other hand, controlled FC stops do not entail this type of risk. Although not all FC abrupt stops can be avoided with an adequate tuning of the system, the total number of abrupt stops and the percentage of abrupt stops with respect to the total number of stops are indicators of the good or bad functioning of the system. The absence of abrupt stops implies no control instabilities and, therefore, a high tuning quality. To measure this, it is important to identify every FC stop and distinguish the abrupt from the controlled ones.

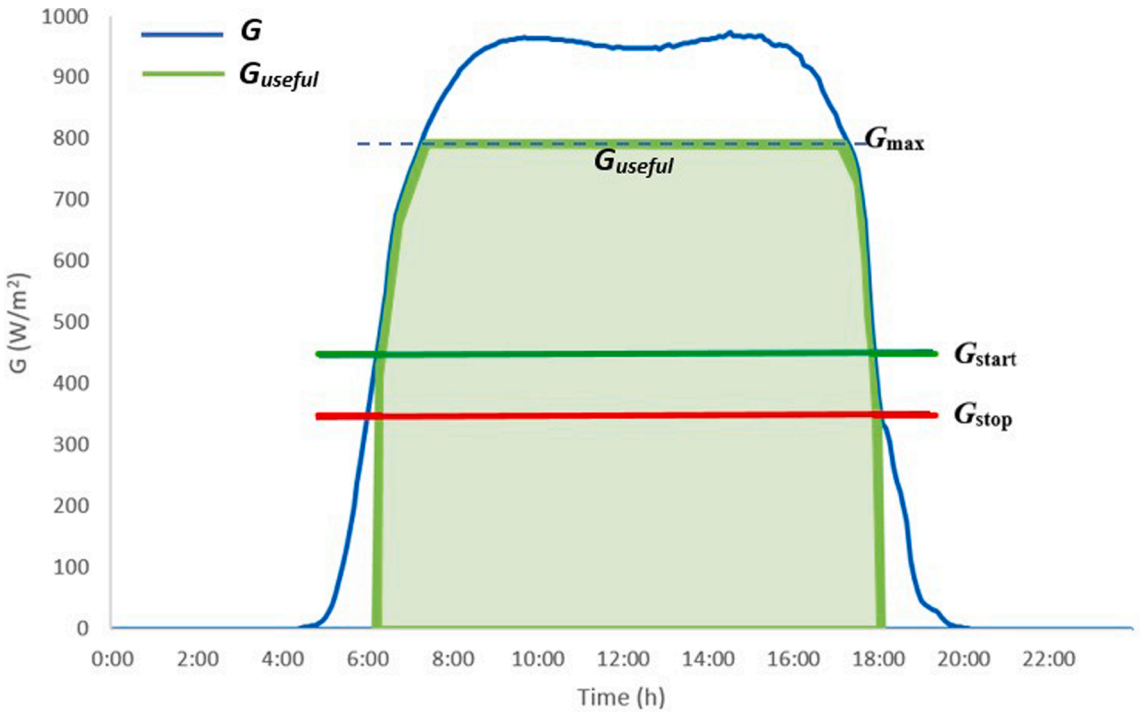

Fig. 8. Graphical representation of the useful irradiance for a PV irrigation system working at a variable frequency.

Passing-cloud resistance ratio

A cloud passing over the PV generator can partially or totally shade it and cause a PV power fluctuation. The effects of the power fluctuation on the PVIS depend on the fluctuation itself and on the characteristics of the PVIS. Not every fluctuation is critical to the operation of the system. For this reason, it is necessary to identify which passing-clouds (understood as PV power fluctuations) are potentially dangerous. The two key characteristics of PV power fluctuations, which affect their potential danger, are power drop (final power minus initial power ΔP_{DC}), and duration (the time, Δt, it takes power to drop). Deep power drops in short periods are likely to cause adverse effects, in terms of abrupt stops, to the PVIS. However, power drop and duration not only depend on the type of cloud (darkness, size and speed), but on the system design (specially the size of the PV generator and the number and arrangement of FCs). Therefore, the target PV power drop and duration to be resisted need to be specified taking into account weather conditions and PVIS design information. As PV power drop information is not always available (for example when there is an abrupt stop), the specification should also consider the irradiance drop that causes it. Beyond these considerations, a first approximation to the definition of a potentially dangerous passing-cloud considers clouds passing over the PV generator at a speed of approximately 70 km/h causing 40% to 50% PV power drops. This means that abrupt stops should be avoided for PV power ramps of duration greater than or equal to $\Delta t(\mathrm{s}) = l(\mathrm{m})/20(\mathrm{m/s})$, where l is the smallest dimension of the perimeter of the PV generator expressed in meters.

To assess whether or not the system resists passing-clouds a passing-cloud resistance ratio (σ_{cloud}) is defined as $\sigma_{cloud} = \#resistedclouds/\#clouds$, where "# resisted clouds" is the number of passing-clouds that do not lead on to FC abrupt stops and "# clouds" is the total number of passing-clouds in a specific period of time.

Performance ratio for PV irrigation systems

Traditionally, to analyse the global performance of PV grid-connected plants, it has been used the *performance ratio* [40], defined as $PR = E_{\mathrm{PV}}/((P^*/G^*)\int G dt)$, where P^* is the peak power of the PV generator, G^* is the irradiance at standard test conditions (1000 W/m^2), G is the irradiance on the plane of PV generator, and E_{PV} is the energy produced by the PV system. Due to the specificities of large-power PVIS, it is interesting to distinguish between PR losses for three different reasons: the non-irrigation period, associated to water needs of the crop; the intrinsic characteristics of the PV system design; and external circumstances that may affect the PR like the irrigation community habits or the different rainfall over time. Equation (1) expresses the PR taking them into consideration [21]:

$$PR = \frac{E_{PV}}{P^*/G^*} \times \frac{1}{\int^G dt} \times \frac{\int_{\mathrm{IP}} G dt}{\int_{\mathrm{IP}} G dt} \times \frac{\int G_{\mathrm{useful}} dt}{\int G_{\mathrm{useful}} dt} \times \frac{\int G_{\mathrm{used}} dt}{\int G_{\mathrm{used}} dt} \quad (1)$$

where:

- IP is the irrigation period determined by either the crop, its water needs and climatic conditions, in case of direct pumping, or by the relation between water needs, pumping capacity and pumped water storage capacity, in case of pumping to a water pool.
- G_{useful} is the available useful irradiance during the IP (the irradiance required to deliver the power needed to pump water). It is determined by the relationship between the PV generator nominal power (P^*), the PV generator supporting structure, and the characteristics of irrigation system. When the available irradiance is below a minimum, the system cannot pump because there is not enough power, and irradiances higher than G_{useful} are partially wasted because the PV generator cannot supply more power than that consumed by the pump working at its nominal power.
- G_{used} is the irradiance effectively used by the system and depends on the number and length of abrupt stops of the FCs and on other external circumstances like the availability of water or the irrigator's decisions about whether to activate the system or not.

Figure 8 shows the graphical representation of G_{useful} for a PVIS working at a variable frequency. The FC starts working when the available power is greater than a start threshold. If the FC has not been started yet and the available irradiance (G) is below the minimum needed to reach the power threshold (G_{start}), the FC cannot be started, the irradiance is wasted and is not considered part of G_{useful}. The same

Table 1
K_c values as a function of t_{acel} and V_{sp}.

t_{acel} (s)	$V_{sp} = 540$ V	$V_{sp} = 550$ V	$V_{sp} = 560$ V
0.8	6.0	6.6	7.4
0.6	6.0	6.4	6.8
0.4	5.8	6.2	6.3

happens once the FC converter is running and G drops below G_{stop} (minimum irradiance level under which the FC cannot be running anymore and is stopped). From that moment on, if the FC stops and G is lower than G_{start}, it will not be part of G_{useful}. In the same way, if the available irradiance is greater than the one that allows the PV generator to provide the maximum power that the pump can consume at a given cell temperature (G_{max}), the difference $G - G_{max}$ will not be part of G_{useful}.

Equation (1) can be rewritten as $PR = PR_{PV} \times UR_{IP} \times UR_{PVIS} \times UR_{EF}$ [21], where:

$$PR_{PV} = \frac{E_{PV}}{P^*/G^*} \times \frac{1}{\int_{used}^{G} dt};$$
$$UR_{IP} = \frac{\int_{IP} Gdt}{\int_{IP} Gdt};$$
$$UR_{PVIS} = \frac{\int G_{useful}dt}{\int_{IP} Gdt}; \quad (2)$$
$$UR_{EF} = \frac{\int G_{used}dt}{\int G_{useful}dt}$$

PR_{PV} is the PR considering only losses strictly related to the PV system itself; UR_{IP} is the utilization ratio related to the irrigation period; UR_{PVIS} is the utilization ratio related to the PVIS design (type of irrigation system, the ratio PV peak power - PV power required for irrigation, the tracking geometry and the accuracy of the PLC control algorithms setup); and UR_{EF} is the utilization ratio related to the irrigator's decisions.

Results of the systematic tuning processes

Aldeanueva

Systematic tuning

To obtain a stable oscillation it is necessary to increase the t_{acel} above its normal operating value (0.1 s). Table 1 shows experimental K_c values obtained for different t_{acel} and V_{sp} values. In all tests, the open circuit voltage (V_{OC}) of the generator is 650 V and the critical period T_{crit} has an approximate value of 275 ms. Fig. 9 shows an example of the oscillation obtained for $t_{acel} = 0.8$ s and $V_{sp} = 560$ V.

Applying the conclusions of section 2.2.1 to the data shown in Table 1, the K_c value obtained under normal operating conditions ($t_{acel} = 0.1$ s and $V_{sp} = 0.8 \cdot V_{OC} = 520$ V) is $K_c \approx 4.4$; $T_c \approx 275ms$

The appropriate value of K_p is obtained by applying the AMIGO tuning rules: $K_p = 0.16 \cdot K_c \approx 0.7$

The results reported in [35] show that the operation of the system presents few changes for T_i values between $0.5 \cdot T_{crit}$ and T_{crit}. According to this, the optimal value of T_i should be between 180 ms and 275 ms. As the resolution of the FC used in this PVIS allows changes of 0.1 s intervals, fine adjustment tests can be carried out for T_i values of 0.1, 0.2 and 0.3 s.

Fine adjustment of the parameters

Although tests were carried out with different values of frequency increments in pump 2, those carried out with a step from 44 Hz to 50 Hz in a time interval of 2 s, which simulate an "aggressive" cloud profile, were analyzed. For T_i values equal to 0.1 s and 0.2 s, undervoltage alarms occurred in the FC of pump 1, so T_i was definitively set at 0.3 s. Table 2 shows the results obtained for various sets of parameters. The best performance correspond to $K_p = 0.5$ and $K_p = 0.6$. The former has a better V_{DCmin} value and the latter optimizes the IAFE. Robustness (higher values of V_{DCmin}) was considered a priority over efficiency (lower values of IAFE), so the selected values for K_p and T_i where 0.5 and 0.3 respectively.

Figure 10 shows the IAFE (shaded area) for a K_p value of 0.8, and Fig. 11 shows the comparison between the generator's voltages (a) and the pump's working frequencies (b) for $K_p = 0.5$ and $K_p = 0.6$.

Villena

Systematic tuning

In this case, stable oscillations were only achieved for t_{acel} greater than 0.8 s, for a value of $V_{sp} = 0.85 \cdot V_{OC} = 544$ V. In contrast to the Aldeanueva facility, the values obtained for K_c and T_{crit} were practically

Table 2
Results for a frequency step from 44 Hz to 50 Hz in 2 s.

K_p	T_i (s)	V_{DCmin} (V)	IAFE (Hz·s)
0.4	0.3	"undervoltage"	
0.5	0.3	474	52.93
0.6	0.3	467	35.17
0.7	0.3	459	37.04
0.8	0.3	462	78.93

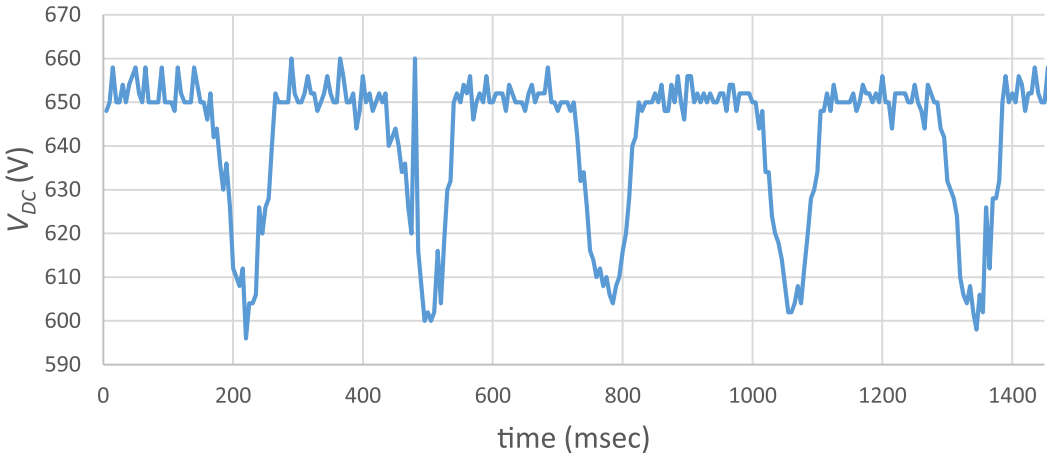

Fig. 9. Critical oscillation in generator voltage.

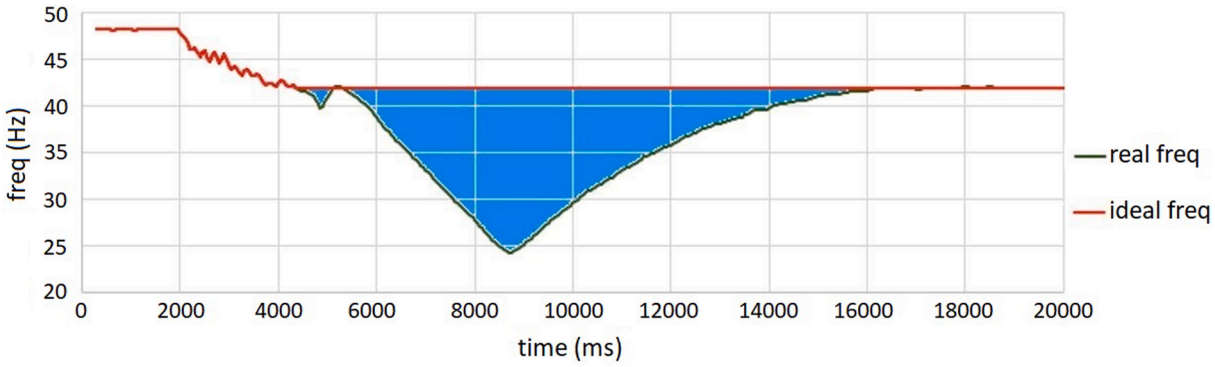

Fig. 10. IAFE (shaded area) for $K_p = 0.8$ and $T_i = 0.3$ s.

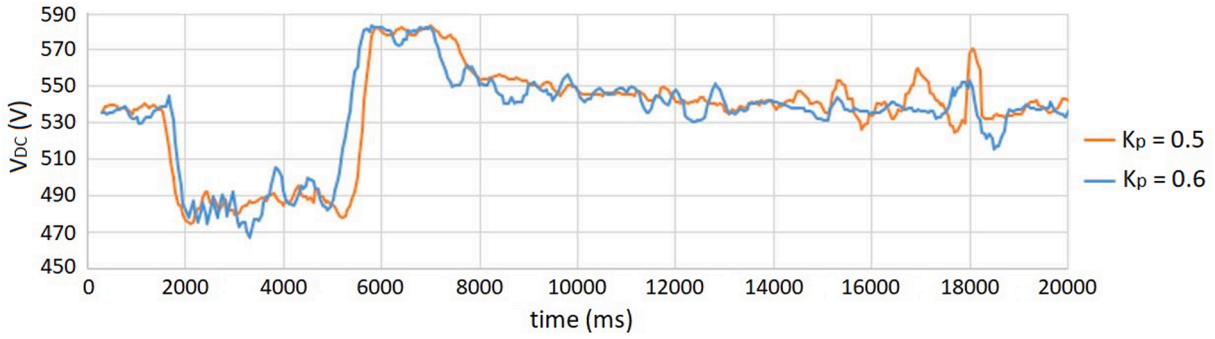

(a)

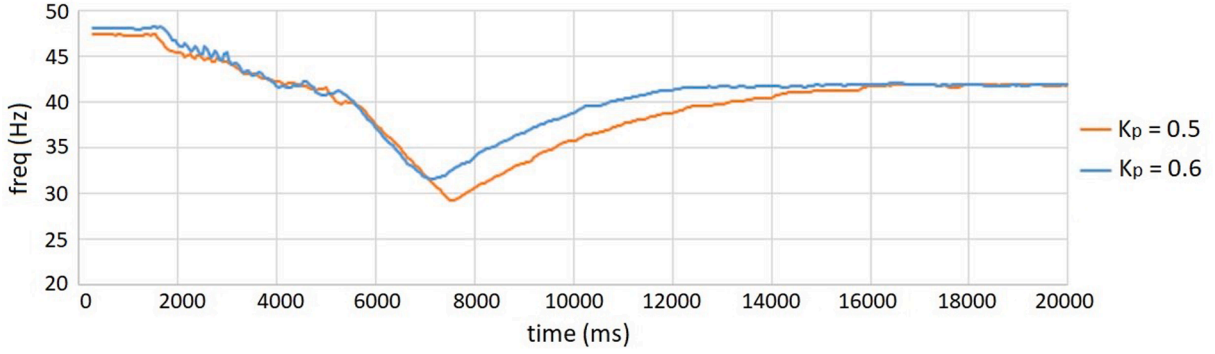

(b)

Fig. 11. V_{DC} (a) and frequency (b) for $K_p = 0.5$, $K_p = 0.6$ and $T_i = 0.3$ s.

Table 3
Critical gain and period for several values of t_{acel}.

t_{acel} (s)	K_c	T_i (ms)
0.8	0.64	101
0.9	0.64	102
1.0	0.64	102

identical ($K_c \approx 0.64; T_c \approx 100$ms) for different acceleration times, as shown in Table 3 and Fig. 12 (oscillation for $t_{acel} = 0.8$ s). Applying the AMIGO rules, the values obtained for K_p and T_i are $K_p = 0.16 \cdot K_c \approx 0.10$; $T_i \in [0.1\text{s}; 0.2\text{s}]$

Fine adjustment of the parameters

The tests were carried out with a 4 Hz frequency increase of the feedforward signal. Regarding its slope, the smallest time interval supported without an undervoltage alarm was 1.6 s. Table 4 shows the results obtained for different control parameters values (only result obtained for the minimum value of the supported time interval have been represented).

It can be concluded that the results obtained for $T_i = 0.1$ s are much better than for $T_i = 0.2$ s. For this value of T_i, K_p values greater than 0.10 were tested, but it was not possible to overcome a ramp with a time less than 1.6 s. Furthermore, as K_p was increased, there were greater oscillations in the generator voltage, so the FC was finally configured using the most conservative values: $K_p = 0.10$ and $T_i = 0.1$ s. As an example, Fig. 13 shows the PV generator voltage and the PID controller output frequency for $K_p = 0.16$; $T_i = 0.2$ s and $K_p = 0.10$; $T_i = 0.1$ s.

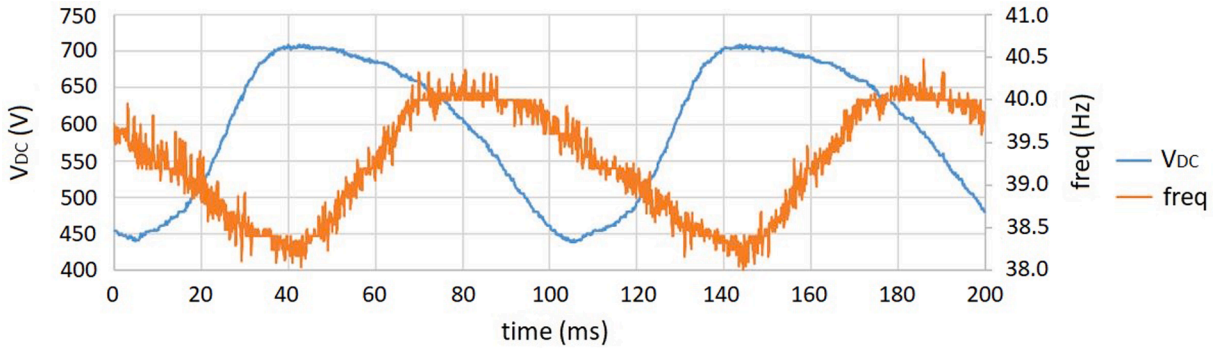

Fig. 12. V_{DC} and frequency curves for critical gain of 0.64 and t_{acel} of 0.8 s.

Table 4
Minimum PV generator voltage and IAE for several sets of control parameters.

K_p	T_i (s)	min interval (s)	V_{DCmin} (V)	IAE (V·s)
0.10	0.2	5.0	532	127
0.11	0.2	4.0	530	113
0.12	0.2	3.0	495	108
0.13	0.2	3.0	526	97
0.14	0.2	2.7	521	92
0.15	0.2	2.5	482	84
0.16	0.2	2.1	518	79
0.09	0.1	2.0	522	78
0.10	0.1	1.6	536	69

Table 5
Number of stops prior to tuning - Villena PVIS.

Year	Month	Days	Stops	Controlled stops	Abrupt stops	Abrupt stops (%)
2019	12	20	94	80	14	14.9
2020	01	26	87	63	24	27.6
	02	29	341	191	150	44.0
	03	30	333	179	154	46.2
Total		105	855	513	342	**40.0**
Total per day		–	**8.1**	**4.9**	**3.3**	–

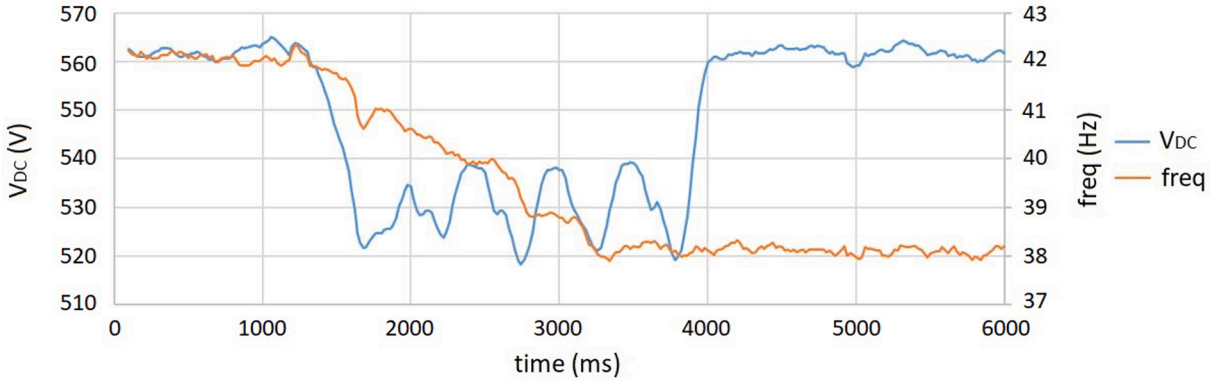

(a)

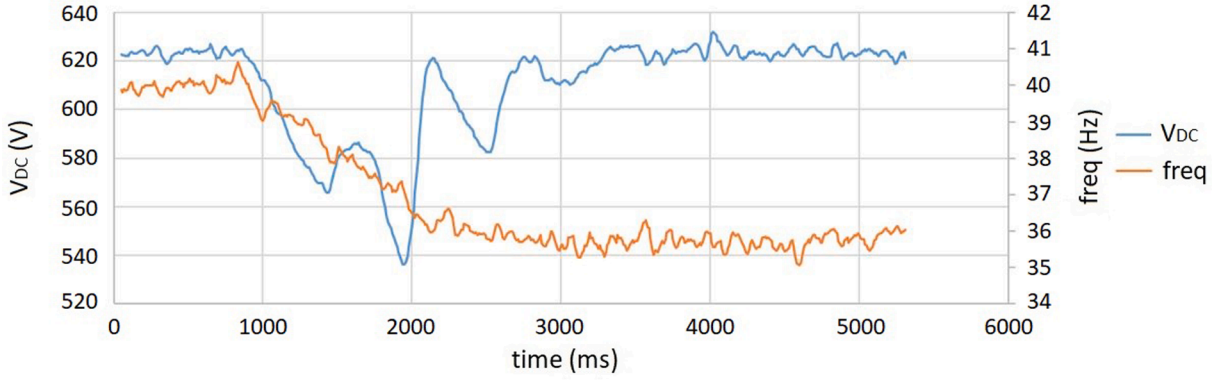

(b)

Fig. 13. PV generator voltage and PID controller output frequency for $K_p = 0.16$; $T_i = 0.2$ s (a) and $K_p = 0.10$; $T_i = 0.1$ s (b).

Table 6
Number of stops after tuning - Villena PVIS.

Year	Month	Days	Stops	Controlled stops	Abrupt stops	Abrupt stops (%)
2020	04	30	211	201	10	4.7
	05	30	226	202	24	10.6
	06	29	283	247	36	12.7
	07	31	146	137	9	6.2
	08	31	171	146	25	14.6
	09	30	196	192	4	2.0
	10	4	34	20	14	41.2
	11	13	52	52	0	0
	12	31	123	123	0	0
2021	01	29	145	143	2	1.4
	02	24	115	115	0	0
Total		282	1702	1578	124	**7.3**
Total per day		–	**6.0**	**5.6**	**0.4**	–

Table 7
Number of stops prior to tuning - Aldeanueva PVIS.

Year	Month	Days	Stops	Controlled stops	Abrupt stops	Abrupt stops (%)
2019	01	31	710	544	166	23.4
	02	28	316	270	46	14.6
	03	31	518	384	134	25.9
	04	30	682	423	259	38.0
	05	31	1391	525	866	62.3
	06	29	902	489	413	45.8
	07	31	587	357	230	39.2
	08	31	268	176	92	34.3
	09	27	369	286	83	22.5
Total		269	5743	3454	2289	**39.8**
Total per day		–	**21.3**	**12.8**	**8.5**	–

Table 8
Number of stops after tuning - Aldeanueva PVIS.

Year	Month	Days	Stops	Controlled stops	Abrupt stops	Abrupt stops (%)
2019	10	28	420	416	4	1.0
	11	30	336	336	0	0.0
	12	31	162	160	2	1.2
2020	01	26	75	75	0	0.0
	02	29	268	264	4	1.5
	03	31	454	437	17	3.7
	04	7	32	27	5	15.6
	05	2	4	4	0	0.0
	06	6	38	38	0	0.0
	07	29	189	184	5	2.6
	08	31	269	265	4	1.5
	09	30	370	369	1	0.3
	10	30	539	537	2	0.4
	11	30	163	163	0	0.0
	12	31	257	255	2	0.8
Total		371	3576	3530	46	**1.3**
Total per day		–	**9.6**	**9.5**	**0.1**	–

Performance results

Number of abrupt stops

Villena

Table 5 and Table 6 show total number of stops per month and per day, considering only days within the IP for which information is available, prior and after tuning[1]. The new tuning methodology has led on to a very important reduction in the number of abrupt stops per day (from 3.3 to 0.4 or an 87.9%). This carries a 25.9% decrease in the total number of stops per day and a 14.3% increase in the number of controlled stops since most system instabilities either do not cause abrupt stops or end up leading on to controlled stops if the instability persists. Prior to the new tuning, more than 40% of the stops where abrupt stops. Post-tuning data show a percentage of abrupt stops less than 7.3%. The low number of days in which the FC starts during October and November 2020 is due to a pump failure and the time it takes to repair it.

Aldeanueva

Table 7 and Table 8 show total number of stops per month and per day, considering only days within the IP for which information is available, before and after tuning. Data show how the new tuning methodology has led on to a 98.8% reduction in the number of abrupt stops per day causing a 54.9% decrease in the total number of stops per day because most system instabilities do not cause abrupt stops. Before applying the new tuning procedure, the percentage of abrupt stops was 39.8%. After the tuning change, it has been reduced to 1.3%. For an adequate analysis of the data, it is important to take into consideration that the number of stops that occur during May and June 2019 increases due to the high number of abrupt stops, caused by a large number of passing clouds, a low passing-cloud resistance ratio and other system instabilities. On the other hand, since April, May and June 2020 do not completely belong to the IP, the number of days considered for those months is very small.

Passing-cloud resistance ratio

In order to calculate the passing-cloud resistance ratio, passing-clouds must be characterized for each system under study. This involves identifying the PV power drop and its duration in the terms described above. To do so, information about the dimensions of the PV generator and weather conditions of the place where it is located is required.

Villena

The smallest dimension of the perimeter of Villena PV generator is 89 m, so the duration of passing-clouds (Δt) should be 4.45 s. Since the system provides logs every second, the duration needs to be rounded to either 4 or 5 s.

To determine the passing-cloud power drop, a study of the existing clouds throughout the months of March, April and May 2020 is made. The study focuses on the PV power drop caused by a cloud passing over the PV generator, but it also includes the irradiance drop information. The PV power drop information is not always available because, when an abrupt stop happens, the PV power goes immediately to zero, but the irradiance information provided by the calibrated cell is. An irradiance

[1] Although Villena monitoring system has been collecting data on a regular basis since May 2017, the stops information shown in the tables starts in December 2019. Previously, the system was storing twenty-seconds records. That is insufficient to calculate the type of stop and to determine if there are passing-clouds or not. On December the 12th, 2019, the monitoring system starts storing one-second records, allowing the calculation of stops and passing-clouds.

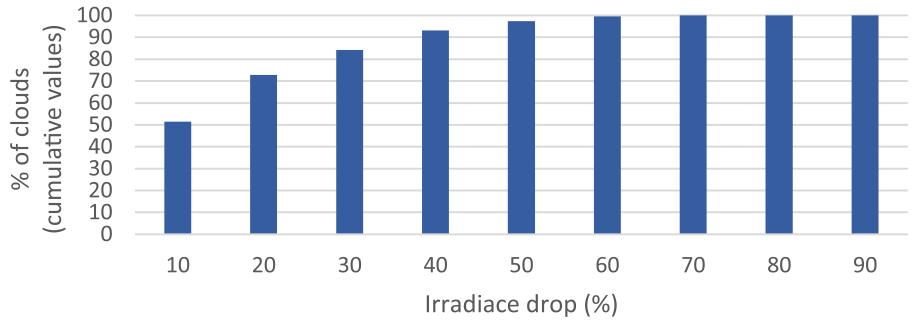

Fig. 14. Cumulative distribution of detected clouds according to irradiance drop - Villena PVIS.

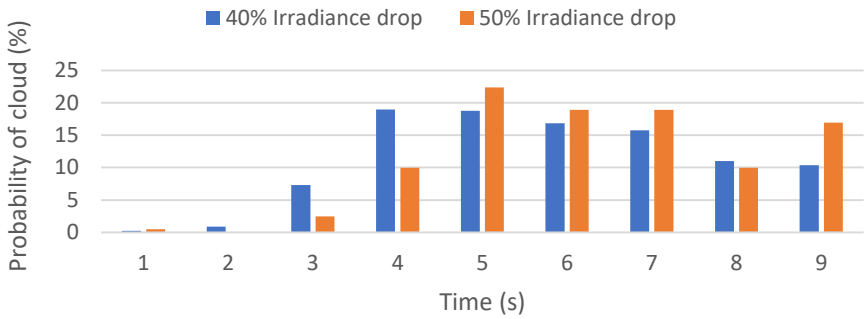

Fig. 15. Probability density function of number of clouds causing 40% (blue) and 50% (orange) irradiance drops as a function of the drop time interval - Villena PVIS. (For interpretation of the references to colour in this figure legend, the reader is referred to the web version of this article.)

Table 9
Monthly passing-cloud resistance ratio prior to tuning (%) - Villena PVIS.

Year	Month	σ_{cloud} (4 s)	σ_{cloud} (3 s)	σ_{cloud} (3 s cum.)
2019	12	60.0	100.0	82.4
2020	01	50.0	50.0	72.7
	02	83.3	75.0	68.4
	03	58.7	34.8	61.7
Total		**61.0**	**46.9**	**65.0**

Table 10
Monthly passing-cloud resistance ratio after tuning (%) - Villena PVIS.

Year	Month	σ_{cloud} (4 s)	σ_{cloud} (3 s)	σ_{cloud} (3 s cum.)
2020	04	83.3	75.0	94.2
	05	94.2	84.6	94.5
	06	98.6	94.1	98.3
	07	96.2	100	99.1
	08	97.2	95.5	98.6
	09	96.7	90.9	98.8
	10	100	100	100
	11	–	–	–
	12	100	100	100
2021	01	100	97,8	99.4
	02	100	100	100
Total		**96.9**	**95.1**	**97.9**

drop identified by the calibrated cell does not necessarily correspond to a PV power drop as the cloud can shade the cell but not a significant part of the PV generator. A filter is applied to consider just irradiance drops causing PV power drops. Under this condition, the percentage of clouds that cause irradiance drops from 10 to 90% in a nine-seconds or less time interval is calculated. Cumulative values are represented in Fig. 14.

93.1% of the clouds that produce equivalent decreases in the irradiance measured by the calibrated cell and in PV power, are associated

Table 11
Monthly passing-cloud resistance ratio prior to tuning (%) - Aldeanueva PVIS.

Year	Month	σ_{cloud} (4 s)	σ_{cloud} (3 s)	σ_{cloud} (3 s cum.)
2019	01	95.7	96.7	93.1
	02	95.7	88.5	93.2
	03	91.2	69.8	86.0
	04	73.8	74.4	78.0
	05	50.0	48.8	52.1
	06	85.3	86.6	82.4
	07	94.1	88.9	89.0
	08	57.1	37.5	51.4
	09	57.1	36.8	64.8
Total		**80.8**	**74.1**	**79.0**

Table 12
Monthly passing-cloud resistance ratio after tuning (%) - Aldeanueva PVIS.

Year	Month	σ_{cloud} (4 s)	σ_{cloud} (3 s)	σ_{cloud} (3 s cum.)
2019	10	100	100	99.4
	11	100	100	100
	12	100	100	100
2020	01	100	–	100
	02	100	100	100
	03	98.6	100	99.3
	04	100	100	95.7
	05	–	–	–
	06	100	100	100
	07	100	100	100
	08	100	100	100
	09	100	100	100
	10	100	100	100
	11	100	100	100
	12	100	100	100
Total		**99.8**	**100**	**99.8**

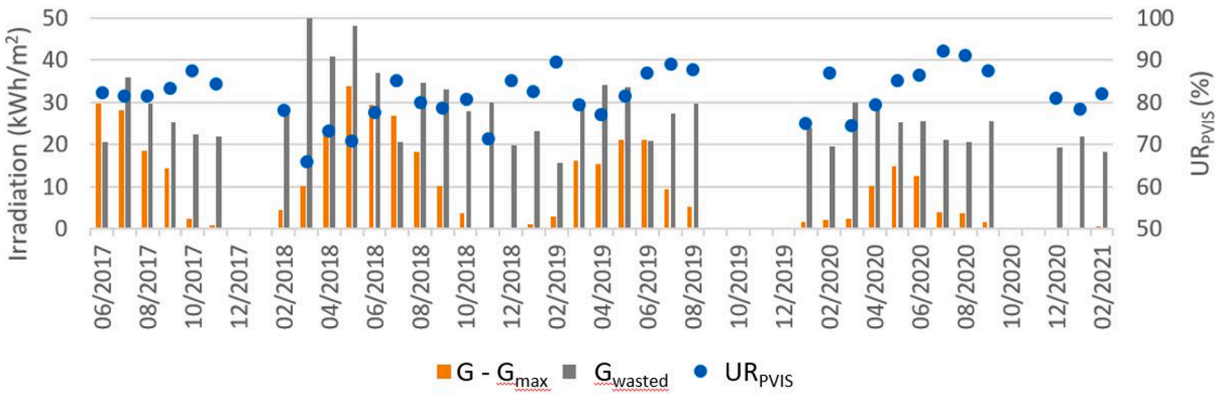

Fig. 16. Evolution of irradiation lost by saturation and wasted by not reaching the start threshold in comparison with the UR_{PVIS} value.

Table 13
Annual real performance indices (%) - Villena PVIS.

Year of operation	PR_{PV}	UR_{IP}	UR_{PVIS}	UR_{EF}	PR
1st (06/2017 to 05/2018)	79.5	100	76.2	96.7	58.5
2nd (06/2018 to 05/2019)	80.0	100	80.9	99.3	64.2
Accumulated prior to tuning	79.7	100	78.5	98.0	61.4
3rd (03/2020 to 02/2021)	75.9	100	85.2	97.4	63.0

Table 14
Annual real performance indices (%) - Aldeanueva PVIS.

Year	PR_{PV}	UR_{IP}	UR_{PVIS}	UR_{EF}	PR
2019 (Prior to tuning)	87.1	100	70.3	98.0	60.0
2020 (After tuning)	86.9	72.4	75.6	98.5	46.8

Table 15
Number of abrupt stops and passing-cloud resistance ratio summary before and after systematic tuning.

	Abrupt stops (%)	
	Prior	After
Villena	40.0	7.3
Aldeanueva	39.8	1.3
	Passing cloud ratio-4 s (%)	
Villena	61.0	96.9
Aldeanueva	80.8	99.8

with 40% (or less) irradiance drops, and 97.4% of the clouds are associated with 50% (or less) irradiance drops. Only 2.6% of the clouds cause 60% irradiance drops and there are no clouds causing higher drops. Under the assumption that if the system resists clouds that cause a 50% irradiance drop, it will also resist clouds that cause smaller drops, it is reasonable to focus the study on this type of clouds.

Furthermore, the irradiance drop slope is analysed for all clouds causing 40% and 50% irradiance drops in a time interval equal to or less than 9 s. Results are classified according to the time it takes the irradiance to drop (Fig. 15). The probability of a 40% irradiance drop starts to grow for clouds with a three-seconds drop interval and reaches its maximum for 4 s clouds. For 50% irradiance drops the curve shifts one second to the right, with a maximum in 5 s clouds. Under the assumption that if the system resists clouds with a shorter drop interval, it will also resist clouds with longer drop intervals, it is reasonable to focus the study on clouds with a four-seconds drop interval.

Cloud analysis results suggest focusing the passing-cloud resistance ratio study on passing-clouds with a 50% power drop and a four-seconds duration, associated with 50% irradiance drops. Using this criterion, the passing-clouds sample is too small. For this reason, it was decided to expand the sample considering 40% power drop passing-clouds with a four-seconds duration, associated with 50% irradiance drops. Passing-clouds with a three-seconds duration are studied as well. Table 9 and Table 10 show the passing-cloud resistance ratio per month before and after tuning, respectively, for these two types of clouds. The cumulative index (considering all passing-clouds with durations from 3 to 9 s) is also shown. Usually, the passing-cloud resistance ratio decreases when the passing-cloud duration decreases and cumulative values are better than 3 and 4 s values since the cumulative ratio includes data from passing-clouds with longer durations, which are resisted more efficiently by the system. This behaviour may not be reflected in the data of a specific month if the number of passing-clouds is low. Finally, tables show a very important σ_{cloud} improvement. For example, σ_{cloud} *(4 s)* ratio after applying the new tuning method improves from 61.0% to 96.9%.

Aldeanueva

The smallest dimension of the perimeter of Aldeanueva PV generator is 74 m, so the duration of passing-clouds (Δt) should be 3.7 s. Since the system provides logs every second, the duration needs to be rounded to either 3 or 4 s.

After an analysis identical to that of Villena, it is observed that 93.7% of the clouds that produce equivalent irradiance and PV power decreases are associated with 40% (or less) irradiance drops, and 97.3% of the clouds are associated with 50% (or less) irradiance drops. The probability of a 40% irradiance drop starts to grow for clouds with a 2 s drop interval and reaches its maximum for 3 and 4 s clouds. In the case of 50% irradiance drops, the maximum is reached for 4 s clouds.

Table 11 and Table 12 show the passing-cloud resistance ratio per month before and after tuning, respectively, for these two types of clouds. The cumulative index (considering passing-clouds with durations from 3 to 9 s) is also shown. Tables show an improvement in the ratio after applying the new tuning method. The global passing-cloud resistance ratio before tuning is 80.8% for four-seconds clouds. After tuning, σ_{cloud} increases to 99.8%.

Performance ratio for PV irrigation systems

Villena

Annual performance indices from June 2017 to February 2021 are shown in Table 13. PR_{PV} suffers a significant decrease after tuning. Its value should be similar to that prior to tuning or slightly lower due to the degradation of PV panels. A lower number of abrupt stops suggests the possibility of a higher PR_{PV} value, but most of the FC abrupt stops that take place between May and August 2020 are not caused by passing clouds but other system instabilities, probably due to pump degradation (in fact, the pump finally broke down on October the 4th, 2020 and had to be repaired), that make the FC stay stopped 10 times longer than

Table 16
Performance indices values summary before and after systematic tuning.

	Performance ratio (%)									
	Prior					After				
	PR_{PV}	UR_{IP}	UR_{PVIS}	UR_{EF}	PR	PR_{PV}	UR_{IP}	UR_{PVIS}	UR_{EF}	PR
Villena	79.7	100	78.5	98.0	61.4	79.2	100	85.2	97.4	65.7
Aldeanueva	87.1	100	70.3	98.0	60.0	86.9	100	75.6	98.5	64.7

when the stop is caused by a passing cloud. These stops have a great impact on PR_{PV}, offsetting its improvement due to the smaller number of abrupt stops. Discounting this negative effect, a 79.2% PR_{PV} is obtained.

UR_{PVIS} values improve at the second operation year due to an increase in the maximum operating frequency from 45.5 Hz to 46.8 Hz at the end of March 2019. This change increases the maximum power supplied by de FC and G_{max} and reduces the waste of energy due to pump saturation ($G - G_{max}$ is lower). Other UR_{PVIS} variations are conditioned by the weather conditions and the number of FC stops. Clear days in which G is smaller than G_{max}, usually clear winter days, make this index to increase. Clear days in which G is bigger than G_{max} and days with passing-clouds make this index to decrease. Fig. 16 shows the evolution of lost irradiation due to saturation and wasted irradiation due to not reaching the start threshold or due to the time interval the FC needs to keep stopped before a new start attempt. Lost irradiation due to saturation is minimal or non-existent since October to February and reaches a maximum in May/June. Similarly, the wasted irradiation due to not reaching the start threshold tends to increase from March to May (months with a high number of controlled stops that keep the FC temporarily stopped).

Table 13 also shows that, after applying the new tuning methodology, there has been a significant improvement in UR_{PVIS} values from 78.5% (accumulated value before tuning) to 85.2% due to weather conditions. This is because the total irradiation lost (due to saturation and the start threshold) between January and August decreases a 4.4% from the second year of operation to the third one (493.3 kWh/m^2 to 471.5 kWh/m^2). UR_{EF} values are close to 100%. The existing difference is due to the irrigator decisions and does not depend on tuning. As an example, on December 2017 and January 2018 a breakdown was detected in the fan used to cool the pumping station and the system was stopped during 30 days to avoid any damage, which explains the lower value during the first year of operation. The PR of the second year of operation reaches a value of 64.2% that is an improvement over the first year due to the increase in the maximum working frequency. After tuning, the PR decreases slightly (63.0%) due to the low PR_{PV}, but reaches 65.7% if the negative effect of abrupt stops due to pump degradation is discounted.

Aldeanueva

Annual performance indices are shown in Table 14. PR_{PV} values are similar to PR values expected for grid-connected PV systems, but the decrease in the number of abrupt stops after tuning (September 2019) does not lead on to a better PR_{PV}. As there are two FCs, many times the system reacts to a FC abrupt stop by starting the other FC, so the impact in PR_{PV} is minimal. UR_{IP} is 100% in 2019 but decreases to 72.4% in 2020 because the April-June interval was no part of the IP (the water pool was full and no irrigating was needed due to weather conditions). UR_{EF} values are close to 100% and the reasons that made the irrigator stop the system and that make UR_{EF} lower have not been identified. UR_{PVIS} values are the most affected by weather conditions and FC controlled stops. The decrease in the number of controlled stops after tuning and the different weather conditions during 2020 have a positive effect on this index. The PR of the second year of operation (46.8%) drops considerably compared to that of the first year (60.0%) due to the effect of UR_{IP}. If this value had been the same as the previous year, the PR would have been 64.7%.

Discussion of the results

Since large-power, stand-alone and battery-free PV irrigation systems are relatively new, there are not enough data in the literature on experimental values of the expected performance in this type of systems. This section discusses the expected values of the different performance indices, which will be useful to establish the thresholds required in the quality control procedures associated with contractual frameworks for the sale and installation of this type of PV irrigation systems.

About the passing-cloud definition and its implication in data collection frequency.

The passing-cloud resistance ratio analysis started under two assumptions that this work has shown to be appropriate: i) if a PVIS resists clouds that cause deep PV power drops, it will also resist clouds that cause smaller drops; and, ii) if a PVIS resists clouds that cause a specific PV power fall in a determined period of time, it will also resist clouds for which the period is longer. Therefore, the analysis can be focused on critical passing-clouds: those related to the target PV power drop and duration to be resisted. Results obtained analysing potentially less dangerous passing-clouds will be better that those considering just the critical ones. Although critical passing-clouds need to be specified taking into account weather conditions and PVIS design information, current experience leads us on to generally characterize them by 40% to 50% irradiance drops, causing 40% PV power drops in a 3 to 5 s interval. Therefore, it is important that monitoring systems collect information every second to be able to do the analysis.

Improvements due to the new tuning method

The analysis of results shows that the new systematic tuning method significantly improves the behaviour of PVIS against PV power quick intermittences by reducing the number of abrupt stops and increasing the passing-cloud resistance ratio, but not the PR_{PV}:

- Villena PVIS presents an 87.9% reduction in the average number of abrupt stops per day after tuning. The percentage of abrupt stops over the total number of stops has decreased an 81.8%. Aldeanueva PVIS has experienced a better improvement: reductions of 98.8% and 96.7% respectively.
- Focusing on 4 s clouds, Villena shows a 96.9% passing-cloud resistance ratio after tuning, improving the previous 61.0%. Aldeanueva's 80.8% before tuning becomes a 99.8% after tuning. Based on these data, it is reasonable to require values greater than 95% in a general specification of this parameter in the framework of quality testing procedures.
- The PR improvement cannot be associated with the new tuning, but is probably due to the weather conditions of the period that has been analysed. The new tuning methodology has no impact on PR_{PV}, that suffers a decrease, due to PV module degradation, from 79.7% to 79.2% after discounting the negative effect of abrupt stops in Villena and from 87.1% to 86.9% in Aldeanueva.

The impact of a proper tuning methodology is evident in terms of abrupt stops and system stability. In this way, water hammer and AC

overvoltage, that seriously threaten the integrity of both the hydraulic and electric components of the PVIS, are avoided.

Expected PR values for large-power PVIS pumping to a water pool

PR_{PV} values for Villena (79.2% once the negative effects described above have been discounted) and Aldeanueva (86.9%) differ considerably from each other. The different PV module operating temperatures, that generate lower temperature losses for Aldeanueva, do not explain that difference (PR_{PV} values under standard test conditions, PR_{PV_STC}, are 85.3% and 95.7% respectively). The difference is probably due to an accident at the very beginning of the system operation caused by wind that could have caused damage to some PV modules. A detailed characterization of the PV generator peak power is pending to confirm it. Anyhow, data show that it is reasonable to expect PR_{PV} values over 80.0%.

UR_{IP} is close to 100% in Villena but it falls to 72.4% in Aldeanueva after tuning because the water pool was full and prevented pumping for 78 days. This fact allows us to conclude that, if the PVIS-water pool set is well dimensioned and/or the needs of the crop are extended for most of the year, UR_{IP} should be very close to 100%.

UR_{PVIS} is intrinsic to the PVIS design and dependent on weather conditions. The results show UR_{PVIS} values between 75.6% and 85.2% after tuning. An adequate adjustment of the PV peak power to the PV power required for irrigation and the accuracy of the PLC control algorithms setup and tuning methodology should lead on to values above 85%.

As UR_{EF} considers the irrigator's decisions, a proper use of the PVIS by the irrigator (PV irrigation centred at midday, maintenance tasks in cloudy days or at night, management of water consumption,…) would lead on to values close to 100%, as seen in our results.

PR_{PV}, UR_{IP}, UR_{PVIS} and UR_{EF} determine PR values. Despite the fact that the low value of UR_{IP} in 2020 negatively affects to Adeanueva PR value (46.8%), if UR_{IP} had been 100% after tuning, and assuming the same values for the rest of factors, the PR would have reached 64.7%. This value and the discounted 65,7% obtained in Villena after tuning make us suggest that it is reasonable to expect PR values of 65% in large-power PVIS pumping to a water pool.

Conclusions

For being a recent innovation, there is a lack of experimental performance of stand-alone large-power PV irrigation systems without batteries. This paper is a contribution to the knowledge of the experimental performance data of two PV irrigation systems pumping to water pools with and without a systematic tuning of their control systems.

First, a systematic method of tuning the PID control of FCs is proposed based on the application of the AMIGO design rules to the method of frequency response tuning. In addition, this systematic method is optimized with the fine adjustment of the PID parameters by two methods that have been developed for two of the main configurations of large-power PV irrigation systems. This systematic method was applied to two PV irrigation systems that, until then, had a "conservative" tuning by means of an experimental trial and error method that ensured stable operation under high and stable solar irradiance levels.

To check the goodness of this automatic tuning, the experimental performance data of both systems before and after this tuning have been compared. To do this, new indices had to be proposed to assess both the robustness of the system to fluctuations in PV power due to "passing clouds" (the "Number of abrupt stops" and the "Passing-cloud resistance ratio") and its performance (by factoring the traditional PR to determine the influence of different factors external to the system, which do not exist in grid-connected PV systems but which do influence stand-alone PV irrigation systems). The proposed factors are the PR_{PV}, UR_{IP}, UR_{PVIS} and UR_{EF}. PR_{PV} assesses the performance quality of the PV system itself, while the three utilization factors measure the effect of the crop irrigation period, the hydraulic irrigation system and user behavior, respectively. The results of these indices, before and after systematic tuning, discounting the negative effect of abrupt stops due to pump degradation and considering an irrigation period covering the whole year, are summarized in Table 15 and Table 16:

Obviously, it will be necessary to confirm these expected values with experimental measurements in other PV irrigation systems with water pools, but these preliminary results can be very valuable to establish the technical thresholds to ensure the technical quality of these systems in the context of quality control procedures associated with contracts for the sale and installation of this type of system.

Another relevant line of future research would be the measurement and analysis of these performance indices in direct PV irrigation systems in which there is no pond and which pump directly into the irrigation network at constant pressure and flow.

Funding

This work has been possible thanks to the funding from the European Union's Horizon 2020 research and innovation programme under grant agreement No 952879, and thanks to the Project MADRID-PV2 (P2018/EMT-4308) funded by the Comunidad de Madrid with the support from ERDF Funds.

CRediT authorship contribution statement

Juan Ignacio Herraiz: Software, Validation, Formal analysis, Investigation, Resources, Data curation, Writing – original draft, Writing – review & editing, Visualization. **José Fernández-Ramos:** Validation, Investigation, Resources, Writing – original draft. **Rita Hogan Almeida:** Methodology, Investigation, Writing – original draft. **Eva María Báguena:** Writing – review & editing, Project administration, Funding acquisition. **Manuel Castillo-Cagigal:** Software, Resources, Data curation, Writing – review & editing. **Luis Narvarte:** Conceptualization, Methodology, Investigation, Resources, Writing – review & editing, Supervision, Project administration, Funding acquisition.

Declaration of Competing Interest

The authors declare that they have no known competing financial interests or personal relationships that could have appeared to influence the work reported in this paper.

References

[1] Langarita R, Sánchez Chóliz J, Sarasa C, Duarte R, Jiménez S. Electricity costs in irrigated agriculture: a case study for an irrigation scheme in Spain. Renew Sustain Energy Rev 2016;68:1008–19. https://doi.org/10.1016/j.rser.2016.05.075.
[2] Abu-Aligah M. Design of photovoltaic water pumping system and compare it with diesel powered pump. Jordan J Mech Ind Eng 2011;5:272–80.
[3] Lorenzo C, Almeida RH, Martínez-Núñez M, Narvarte L, Carrasco LM. Economic assessment of large power photovoltaic irrigation systems in the ECOWAS region. Energy 2018;155:992–1003. https://doi.org/10.1016/j.energy.2018.05.066.
[4] Alonso Abella M, Lorenzo E, Chenlo F. PV water pumping systems based on standard frequency converters. Prog Photovoltaics Res Appl 2003;11(3):179–91. https://doi.org/10.1002/pip.475.
[5] Sontake VC, Kalamkar VR. Solar photovoltaic water pumping system - A comprehensive review. Renew Sustain Energy Rev 2016;59:1038–67. https://doi.org/10.1016/j.rser.2016.01.021.
[6] Posorski R. Photovoltaic water pumps, an attractive tool for rural drinking water supply. Sol Energy 1996;58(4-6):155–63.
[7] EIP-Water. Priority area P30: water-energy nexus. European innovation partnership on water boosting opportunities – innovating water. 2013. https://watereurope.eu/tag/eip-water/ (accessed April 1, 2021).
[8] Ismaier A, Schlücker E. Fluid dynamic interaction between water hammer and centrifugal pumps. Nucl Eng Des 2009;239(12):3151–4. https://doi.org/10.1016/j.nucengdes.2009.08.028.
[9] Achouri R, Nouicer O, Mhiri H, Bournot P. Probable cause analysis of cracks observed on vertical centrifugal pump. Eng Fail Anal 2013;29:1–11. https://doi.org/10.1016/j.engfailanal.2012.11.003.

[10] Khiareddine A, Ben Salah C, Mimouni MF. Power management of a photovoltaic/battery pumping system in agricultural experiment station. Sol Energy 2015;112:319–38. https://doi.org/10.1016/j.solener.2014.11.020.
[11] Das M, Mandal R. A comparative performance analysis of direct, with battery, supercapacitor, and battery-supercapacitor enabled photovoltaic water pumping systems using centrifugal pump. Sol Energy 2018;171:302–9. https://doi.org/10.1016/j.solener.2018.06.069.
[12] Bhayo BA, Al-Kayiem HH, Gilani SI. Assessment of standalone solar PV-Battery system for electricity generation and utilization of excess power for water pumping. Sol Energy 2019;194:766–76. https://doi.org/10.1016/j.solener.2019.11.026.
[13] Ghalambaz M, Zhang J. Conjugate solid-liquid phase change heat transfer in heatsink filled with phase change material-metal foam. Int J Heat Mass Transf 2020;146:118832. https://doi.org/10.1016/j.ijheatmasstransfer.2019.118832.
[14] Ghalambaz M, Chamkha AJ, Wen D. Natural convective flow and heat transfer of Nano-Encapsulated Phase Change Materials (NEPCMs) in a cavity. Int J Heat Mass Transf 2019;138:738–49. https://doi.org/10.1016/j.ijheatmasstransfer.2019.04.037.
[15] Fernández-Ramos J, Narvarte-Fernández L, Poza-Saura F. Improvement of photovoltaic pumping systems based on standard frequency converters by means of programmable logic controllers. Sol Energy 2010;84(1):101–9. https://doi.org/10.1016/j.solener.2009.10.013.
[16] Bione J, Vilela OC, Fraidenraich N. Comparison of the performance of PV water pumping systems driven by fixed, tracking and V-trough generators. Sol Energy 2004;76(6):703–11. https://doi.org/10.1016/j.solener.2004.01.003.
[17] Narvarte L, Lorenzo E. Tracking and ground cover ratio. Prog Photovoltaics Res Appl 2008;16(8):703–14. https://doi.org/10.1002/pip.847.
[18] Narvarte L, Fernández-Ramos J, Martínez-Moreno F, Carrasco LM, Almeida RH, Carrêlo IB. Solutions for adapting photovoltaics to large power irrigation systems for agriculture. Sustain Energy Technol Assessments 2018;29:119–30. https://doi.org/10.1016/j.seta.2018.07.004.
[19] Almeida RH, Narvarte L, Lorenzo E. PV arrays with delta structures for constant irradiance daily profiles. Sol Energy 2018;171:23–30. https://doi.org/10.1016/j.solener.2018.06.066.
[20] MASLOWATEN. MASLOWATEN H2020 project. 2016. http://maslowaten.eu/ (accessed April 1, 2021).
[21] Almeida RH, Carrêlo IB, Lorenzo E, Narvarte L, Fernández-Ramos J, Martínez-Moreno F, et al. Development and test of solutions to enlarge the power of PV irrigation and application to a 140 kW PV-diesel representative case. Energies 2018;11(12):3538. https://doi.org/10.3390/en11123538.
[22] Todde G, Murgia L, Carrelo I, Hogan R, Pazzona A, Ledda L, et al. Embodied energy and environmental impact of large-power stand-alone photovoltaic irrigation systems. Energies 2018;11(8):2110. https://doi.org/10.3390/en11082110.
[23] Todde G, Murgia L, Deligios PA, Hogan R, Carrelo I, Moreira M, et al. Energy and environmental performances of hybrid photovoltaic irrigation systems in Mediterranean intensive and super-intensive olive orchards. Sci Total Environ 2019;651:2514–23. https://doi.org/10.1016/j.scitotenv.2018.10.175.
[24] Carrêlo IB, Almeida RH, Narvarte L, Martinez-Moreno F, Carrasco LM. Comparative analysis of the economic feasibility of five large-power photovoltaic irrigation systems in the Mediterranean region. Renew Energy 2020;145:2671–82. https://doi.org/10.1016/j.renene.2019.08.030.
[25] Åström KJ, Hägglund T. Revisiting the Ziegler-Nichols step respose method for PID control. J Process Control 2004;14:635–50.
[26] Cohen GH, Coon GA. Theoretical consideration of related control. Trans ASME 1953;75:827–34.
[27] Chien KL, Hrones JA, Reswick JB. On the automatic Control of generalized passive systems. Trans ASME 1952:175–85.
[28] Hägglund T, Åström KJ. Revisiting the Ziegler-Nichols tuning rules for PI control. Asian J Control 2002;4:354–80. https://doi.org/10.1111/j.1934-6093.2002.tb00076.x.
[29] Hägglund T, Åström KJ. Revisiting the Ziegler-Nichols tuning rules for pi control - Part II The frequency response method. Asian J Control 2004;6:469–82. https://doi.org/10.1111/j.1934-6093.2004.tb00368.x.
[30] Hambali N, Masngut A, Ishak AA, Janin Z. Process controllability for flow control system using Ziegler-Nichols (ZN), Cohen-Coon (CC) and Chien-Hrones-Reswick (CHR) tuning methods. IEEE Int Conf Smart Instrumentation Meas Appl ICSIMA 2014:1–6. https://doi.org/10.1109/ICSIMA.2014.7047432.
[31] O'Dwyer A. Handbook of PI and PID controller tuning rules. third ed. London: Imperial College Press; 2009. https://doi.org/10.1142/P575.
[32] Ziegler JG, Nichols NB. Optimum settings for automatic controllers. Trans ASME 1942;64:759–68. https://doi.org/10.1115/1.2899060.
[33] Åström KJ, Hägglund T. Advanced PID control. IEEE Control Syst Mag 2006;26:98–101. https://doi.org/10.1109/MCS.2006.1580160.
[34] Brito AU, Zilles R. Systematized procedure for parameter characterization of a variable-speed drive used in photovoltaic pumping applications. Prog Photovoltaics Res Appl 2006;14(3):249–60. https://doi.org/10.1002/pip.666.
[35] Fernández-Ramos J, Narvarte L, López-Soria R, Almeida RH, Carrêlo IB. An assessment of the proportional-integral control tuning rules applied to photovoltaic irrigation systems based on standard frequency converters. Sol Energy 2019;191:468–80. https://doi.org/10.1016/j.solener.2019.09.021.
[36] Vick BD, Clark RN. Experimental investigation of solar powered diaphragm and helical pumps. Sol Energy 2011;85(5):945–54. https://doi.org/10.1016/j.solener.2011.02.011.
[37] Belgacem BG. Performance of submersible PV water pumping systems in Tunisia. Energy Sustain Dev 2012;16(4):415–20. https://doi.org/10.1016/j.esd.2012.10.003.
[38] Mohammedi A, Mezzai N, Rekioua D, Rekioua T. Impact of shadow on the performances of a domestic photovoltaic pumping system incorporating an MPPT control: a case study in Bejaia, North Algeria. Energy Convers Manag 2014;84:20–9. https://doi.org/10.1016/j.enconman.2014.04.008.
[39] Benghanem M, Daffallah KO, Alamri SN, Joraid AA. Effect of pumping head on solar water pumping system. Energy Convers Manag 2014;77:334–9. https://doi.org/10.1016/j.enconman.2013.09.043.
[40] Luque A, Hegedus S. Handbook of Photovoltaic Science and Engineering. Chichester: Johm Wiley & Sons; 2003. https://doi.org/10.1002/9780470974704.